

# Significant Effect of Salt Bridges on Electron Transfer

James P. Kirby, James A. Roberts, and Daniel G. Nocera\*

Contribution from the Department of Chemistry, Michigan State University,  
East Lansing, Michigan 48824

Received January 21, 1997<sup>⊗</sup>

**Abstract:** Photoinduced electron transfer within donor–(salt bridge)–acceptor complexes has been investigated. We now report the first comparative study of electron transfer through an asymmetric salt bridge interface formed from the 1:1 association of an amidinium to a carboxylate via two hydrogen bonds. Laser flash excitation prompts an electron to transfer from a highly reducing excited state of a derivatized Ru(II) bipyridine donor complex to a dinitrobenzene acceptor juxtaposed by the salt bridge interface. The rate of electron transfer through the D–(amidinium–carboxylate)–A salt bridge is  $\sim 10^2$  times slower than that for the pair when the interface is switched, D–(carboxylate–amidinium)–A. This large difference shows that a salt bridge can significantly influence the kinetics of electron transfer and, accordingly, bears considerably on electron transport within the biological milieu of proteins and enzymes.

## Introduction

Protons can significantly affect the rates of biological electron transfer. Many proteins and enzymes derive their function by mediating the rates of electron transfer by a proton. Nowhere is this better demonstrated than in the active site of cytochrome *c* oxidase. Although the distances separating the two heme centers from the binuclear Cu<sub>A</sub> centers are similar, electron transfer to heme *a* is  $10^2$ – $10^4$  times faster than that to heme *a*<sub>3</sub>.<sup>1</sup> Proton transfer accompanying heme reduction is believed to be the origin of the slow electron transfer and, accordingly, the controlling factor for directional electron transport via heme *a*.<sup>2</sup> Such proton-coupled electron transfer (PCET) events continue to emerge in the structure/function relations of a variety of other proteins and enzymes, including photosystem II,<sup>3–5</sup> nitrogenase,<sup>6,7</sup> non-heme-iron-containing proteins,<sup>8,9</sup> multicopper oxidases,<sup>10</sup> and reductases<sup>11–13</sup> to name a few. Nevertheless, despite the importance of PCET in the bioenergetic conversion

processes of this diverse biological machinery, the mechanistic details of how the electron couples to the proton remain largely undefined.

To better understand the relationship between electron transfer and proton motion, we have developed an approach to photoinduce electron transfer within a donor–acceptor pair juxtaposed by a proton transfer interface. As we have shown for the symmetric  $-(\text{COOH})_2-$  interface,<sup>14</sup> the overall perturbation of proton motion on electron transfer is small, and electron transfer is fast. Within this interface, proton displacement on one side of the dicarboxylic acid interface is compensated by displacement of a proton from the other side. Because charge redistribution within this interface is negligible, the only mechanism available to engender PCET is the dependence of the electronic coupling on the position of the protons within the interface.<sup>15</sup> Similar results are obtained for acceptor–donor pairs separated by guanine–cytosine base pairs,<sup>16</sup> where the p*K*<sub>a</sub>s of the bases cannot accommodate proton transfer within the interface. These cases, however, are unusual in biology, where protons are typically displaced in a redox process. The coupling of the charge shift that accompanies electron *and* proton motion to the polarization of the surrounding environment may provide a unique mechanism for PCET in biology.<sup>17</sup> Consequently, we have extended our approach to explore PCET reactions mediated by a salt bridge, where changes in polarity, charge, and energetics resulting from the transfer of an electron from the donor to the acceptor are augmented by proton displacement within the salt bridge interface.

The guanidinium–carboxylate interaction afforded by aspartate (Asp)–arginine (Arg) salt bridges offers a platform for the assembly of donor–(salt bridge)–acceptor complexes. This salt bridge is the important stabilizing structural element in many natural systems including RNA stem loops,<sup>18</sup> zinc finger/

\* To whom correspondence should be addressed. Present address: Department of Chemistry 6-335, 77 Massachusetts Ave., Massachusetts Institute of Technology, Cambridge, MA 02139-4307.

<sup>⊗</sup> Abstract published in *Advance ACS Abstracts*, September 15, 1997.  
(1) Ramirez, B. E.; Malmström, B. G.; Winkler, J. R.; Gray, H. B. *Proc. Natl. Acad. Sci. U.S.A.* **1995**, *92*, 11949.

(2) Brzezinski, P. *Biochemistry* **1996**, *35*, 5611.

(3) (a) Graige, M. S.; Paddock, M. L.; Bruce, J. M.; Feher, G.; Okamura, M. Y. *J. Am. Chem. Soc.* **1996**, *118*, 9005. (b) Okamura, M. Y.; Feher, G. *Annu. Rev. Biochem.* **1992**, *61*, 861.

(4) Takahashi, E.; Maroti, P.; Wraight, C. In *Electron and Proton Transfer in Chemistry and Biology*; Müller, A., Ratajczaks, H., Junge, W., Diemann, E., Eds.; Elsevier: Amsterdam, 1992; p 219.

(5) Babcock, G. T.; Barry, B. A.; Debus, R. J.; Hoganson, C. W.; Atamian, M.; McIntosh, L.; Sithole, I.; Yocum, C. F. *Biochemistry* **1989**, *28*, 9557.

(6) Burgess, B. K.; Lowe, D. J. *Chem. Rev.* **1996**, *96*, 2983.

(7) (a) Pilato, R. S.; Stiefel, E. I. In *Bioinorganic Catalysis*; Reedijk, J., Ed.; Dekker: New York, 1993; p 131. (b) Stiefel, E. I. In *Molybdenum Enzymes, Cofactors, and Model Systems*; ACS Symposium Series 535; Stiefel, E. I., Coucouvanis, D., Newton, W. E., Eds.; American Chemical Society: Washington, DC, 1993; p 1. (c) Stiefel, E. I. *Proc. Natl. Acad. Sci. U.S.A.* **1973**, *70*, 988.

(8) Feig, A. L.; Lippard, S. J. *Chem. Rev.* **1994**, *94*, 759.

(9) Wallar, B. J.; Lipscomb, J. D. *Chem. Rev.* **1996**, *96*, 2625.

(10) Solomon, E. I.; Sundaram, U. M.; Machonkin, T. E. *Chem. Rev.* **1996**, *96*, 2563.

(11) (a) Uhlin, U.; Eklund, H. *Nature* **1994**, *370*, 533. (b) Nordlund, P.; Eklund, H. *J. Mol. Biol.* **1993**, *232*, 123.

(12) Ekberg, M.; Sahlin, M.; Eriksson, M.; Sjöberg, B.-M. *J. Biol. Chem.* **1996**, *271*, 20655.

(13) Averill, B. A. *Chem. Rev.* **1996**, *96*, 2951.

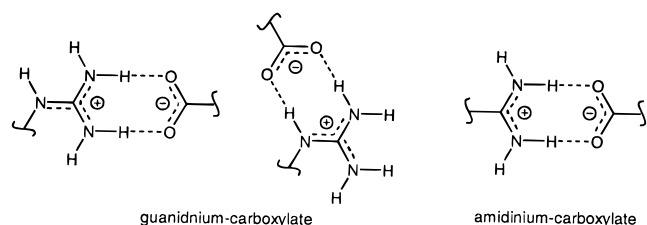
(14) Turró, C.; Chang, C. K.; Leroi, G. E.; Cukier, R. I.; Nocera, D. G. *J. Am. Chem. Soc.* **1992**, *114*, 4013.

(15) Cukier, R. I. *J. Phys. Chem.* **1995**, *99*, 945.

(16) (a) Sessler, J. L.; Wang, B.; Harriman, A. *J. Am. Chem. Soc.* **1993**, *115*, 10418. (b) Harriman, A.; Kubo, Y.; Sessler, J. L. *J. Am. Chem. Soc.* **1992**, *114*, 388. (c) Berman, A.; Izraeli, E. S.; Levanon, H.; Wang, B.; Sessler, J. L. *J. Am. Chem. Soc.* **1995**, *117*, 8252. (d) Sessler, J. L.; Wang, B.; Springs, S. L.; Brown, C. T. In *Comprehensive Supramolecular Chemistry*; Murakami, Y., Ed.; Pergamon Press: Oxford, UK, 1997; Vol. 4, Chapter 9.

(17) (a) Cukier, R. I. *J. Phys. Chem.* **1996**, *100*, 15428. (b) Cukier, R. I. *J. Phys. Chem.* **1995**, *99*, 16101.

Chart 1



DNA complexes,<sup>19,20</sup> and the active sites of dihydrofolate reductase,<sup>21</sup> cytochrome *c* oxidase,<sup>1,2</sup> and siroheme sulfite reductase (SiRHP).<sup>22</sup> For the latter, salt bridge function extends beyond a structural role by establishing a proton channel at the active site to effect the six-electron, six-proton reduction of sulfite to sulfide and water. While the overall structure of a guanidinium-carboxylate interface is ideal for supporting proton transport along an electron transfer pathway, the interface muddles PCET investigations because, as shown in Chart 1, guanidinium presents multiple bonding modes to carboxylate. Kinetics measurements of donor-acceptor pairs bridged by guanidinium-carboxylate may, therefore, be complicated by multiple equilibria. We have reduced the complexity of the problem by employing an amidinium-carboxylate salt bridge, which retains the two N-H bonds of the guanidinium-carboxylate salt bridge while preserving only one specific binding mode for carboxylate. The two-point hydrogen bond of the amidinium-carboxylate interface features two favorable secondary interactions,<sup>23</sup> supported by the electrostatic stabilization of proximate opposite charges within the salt bridge. Accordingly, the amidinium-carboxylate interface readily forms and persists in solutions, even when the dielectric constant of the solvent is high. General procedures for the preparation of amidine from nitrile in high yields have allowed us to efficiently construct the interface on a variety of metal complex and porphyrin donors and acceptors,<sup>24</sup> affording us a wide range of systems for PCET studies.

A direct experimental measure of the affect of a salt bridge on electron transfer is to undertake a comparative kinetics study of a donor-(amidinium-carboxylate)-acceptor supramolecule and its switched interface donor-(carboxylate-amidinium)-acceptor congener. We now report such a study for the supramolecular series of complexes where the donor is [(tmbpy)<sub>2</sub>Ru<sup>II</sup>(Meby-amH<sup>+</sup>)]<sup>3+</sup> or [(tmbpy)<sub>2</sub>Ru<sup>II</sup>(Meby-COO<sup>-</sup>)]<sup>+</sup> (tmbpy = 3,3',4,4'-tetramethyl-2,2'-bipyridine, Meby-amH<sup>+</sup> = 4-methyl-2,2'-bipyridine-4'-amidinium, Meby-COO<sup>-</sup> = 4-methyl-2,2'-bipyridine-4'-carboxylate) and the acceptor is the complementary carboxylate- or amidinium-modified 3,5-dinitrobenzene (**1** and **2**, respectively in Table 1). To further extend the study, we have also prepared the same donor-acceptor pair bridged by the symmetric -(COOH)<sub>2</sub>- interface (**3**). Electron transfer measurements of this series of complexes reveal that the salt bridge can extraordinarily influence the rates of electron transfer,

(18) Puglisi, J. D.; Chen, L.; Frankel A. D.; Williamson, J. R. *Proc. Natl. Acad. Sci. U.S.A.* **1993**, *90*, 3680.

(19) Pavletich, N. P.; Pabo, C. O. *Science* **1991**, *252*, 809

(20) Berg, J. M. *Acc. Chem. Res.* **1995**, *28*, 14.

(21) Howell, E. H.; Villafranca, J. E.; Warren, M. S.; Oatley, S. J.; Kraut, J. *Science* **1986**, *231*, 1125.

(22) Crane, B. R.; Siegel, L. M.; Getzoff, E. D. *Science* **1995**, *270*, 59.

(23) (a) Pranata, J.; Wierschke, S. G.; Jorgensen, W. L. *J. Am. Chem. Soc.* **1991**, *113*, 2810. (b) Jorgensen, W. L.; Pranata, J. *J. Am. Chem. Soc.* **1990**, *112*, 2008.

(24) (a) Roberts, J. A.; Kirby, J. P.; Nocera, D. G. *J. Am. Chem. Soc.* **1995**, *117*, 8051. (b) Kirby, J. P.; van Dantzig, N. A.; Chang, C. K.; Nocera, D. G. *Tetrahedron Lett.* **1995**, *36*, 3477. (c) Deng, Y.; Roberts, J. A.; Peng, S. M.; Chang, C. K.; Nocera, D. G. *Angew. Chem., Int. Ed. Engl.*, in press. (d) Roberts, J. A.; Kirby, J. P.; Wall, S. T.; Nocera, D. G. *Inorg. Chim. Acta*, in press.

thereby allowing us to uncover new contributing effects to the mechanism of biologically relevant PCET.

## Experimental Section

### Materials. Synthesis of 4-Methyl-2,2'-bipyridine-4'-amidinium.

The ligand synthesis began with the preparation of 4-methyl-2,2'-bipyridine-4'-carbonitrile. Hydroxylamine hydrochloride (1.8 g, 26 mmol) was added to a 40 mL formic acid solution of 4-methyl-2,2'-bipyridine-4'-carboxaldehyde<sup>25</sup> (4.0 g, 20 mmol). The solution was refluxed for 24 h under an argon atmosphere. Upon cooling to room temperature, the solution was poured into 200 mL of ice. Neutralization with an aqueous sodium carbonate solution produced a white precipitate, which was extracted into dichloromethane (3 × 50 mL). The organic extracts were combined and dried over magnesium sulfate, and the solvent was removed under reduced pressure to give the product, 4-methyl-2,2'-bipyridine-4'-carbonitrile: yield 3.15 g, 80%; MS 195.1 *m/z*; mp 134–137 °C; <sup>1</sup>H NMR (CD<sub>3</sub>CN) 8.79 (1H, d), 8.60 (1H, s), 8.50 (1H, d), 8.21 (1H, s), 7.62 (1H, d), 7.25 (1H, d), 2.12 ppm (3H, s); <sup>13</sup>C NMR (CD<sub>3</sub>CN) 158.16, 154.76, 151.16, 150.23, 149.82, 126.68, 126.15, 123.54, 122.58, 122.03, 117.76, 21.22 ppm.

Conversion to the amidinium was achieved by charging a solution of freshly prepared sodium methoxide in methanol (20 mL, 0.04 M) with 4-methyl-2,2'-bipyridine-4'-carbonitrile (1.50 g, 7.7 mmol) under argon. The resulting solution was stirred at room temperature for 24 h, ammonium chloride (0.43 g, 8.0 mmol) was added in one portion, and stirring was continued for an additional 24 h under argon. Large colorless crystals of 4-methyl-2,2'-bipyridine-4'-amidinium chloride (yield 0.70 g, 71%) were collected and dissolved in a minimal amount of water. The conversion of the Cl<sup>-</sup> salt to the PF<sub>6</sub><sup>-</sup> salt was quantitative upon the addition of a saturated aqueous solution of ammonium hexafluorophosphate to an aqueous solution of 4-methyl-2,2'-bipyridine-4'-amidinium chloride: MS 212.1 *m/z*; <sup>1</sup>H NMR (CD<sub>3</sub>CN) 8.87 (1H, d), 8.65 (1H, s), 8.52 (1H, d), 8.27 (1H, s), 8.02 (4H, s), 7.64 (1H, d), 7.39 (1H, d), 2.41 ppm (3H, s); <sup>13</sup>C NMR (CD<sub>3</sub>CN) δ 166.79, 158.25, 154.82, 151.51, 150.21, 137.12, 126.82, 122.93, 122.44, 119.84, 21.26 ppm.

**Synthesis of [(tmbpy)<sub>2</sub>Ru(Meby-amH<sup>+</sup>)][(PF<sub>6</sub>)<sub>3</sub>].** The ligand 4-methyl-2,2'-bipyridine-4'-amidinium chloride (0.09g, 0.36 mmol) was reacted with (tmbpy)<sub>2</sub>Ru<sup>II</sup>Cl<sub>2</sub><sup>26</sup> (0.30 g, 0.50 mmol) in refluxing 95% ethanol (20 mL) for 4 h. After the solvent was removed under reduced pressure, the resulting solid was dissolved in a minimal amount of water and filtered. Addition of an aqueous saturated solution of NH<sub>4</sub>PF<sub>6</sub> yielded [(tmbpy)<sub>2</sub>Ru<sup>II</sup>(Meby-amidinium)]<sup>3+</sup> as its PF<sub>6</sub><sup>-</sup> salt, which was washed with water (5 × 15 mL), dried in air, and washed with anhydrous ethyl ether (5 × 15 mL): yield 0.17 g, 40%; ES/MS [M]<sup>2+</sup> 369.6 *m/z*; <sup>1</sup>H NMR (DMSO-*d*<sub>6</sub>) 9.60 (2H, s), 9.37 (2H, s), 9.03 (1H, s), 8.71 (1H, s), 8.59 (4H, s), 7.97 (1H, d), 7.70 (1H, d), 7.59 (1H, d), 7.42 (1H, d), 7.29 (1H, s), 7.28 (1H, s), 7.26 (1H, s), 7.17 (1H, s), 2.55 (3H, s), 2.41 (12H, s), 2.08 ppm (12H, s).

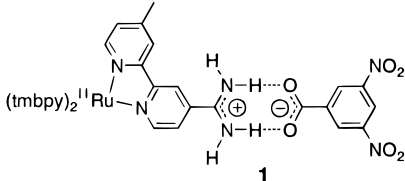
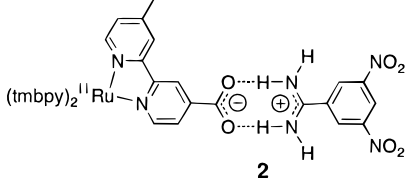
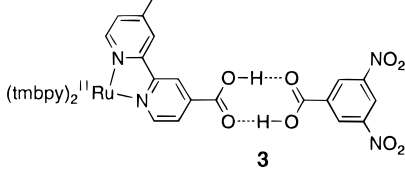
**Synthesis of [(tmbpy)<sub>2</sub>Ru(Meby-COOH)][(PF<sub>6</sub>)<sub>2</sub>] and [(tmbpy)<sub>2</sub>Ru(Meby-COO<sup>-</sup>)][(PF<sub>6</sub>)<sub>2</sub>].** A 95% ethanol (20 mL) solution containing 4-methyl-2,2'-bipyridine-4'-carboxylic acid<sup>25</sup> (0.05 g, 0.23 mmol) and (tmbpy)<sub>2</sub>Ru<sup>II</sup>Cl<sub>2</sub> (0.24 g, 0.39 mmol) was refluxed for 24 h. The solution was cooled and the solvent removed under reduced pressure. The remaining solid was dissolved in a minimal amount of water and filtered. The orange PF<sub>6</sub><sup>-</sup> salt of [(tmbpy)<sub>2</sub>Ru<sup>II</sup>(Meby-COOH)]<sup>2+</sup> was obtained upon the addition of an aqueous saturated solution of NH<sub>4</sub>PF<sub>6</sub>. The product was further purified by charging a column of neutral alumina, activity 1, with a solution of the complex salt and eluting with dichloromethane and ethanol (6:1 v/v): yield 0.12 g, 52%; ES/MS [M]<sup>2+</sup> 370.0 *m/z*; <sup>1</sup>H NMR (CD<sub>3</sub>CN) 8.89 (1H, s), 8.45, (1H, s), 8.27, (4H, m), 7.72 (1H, d), 7.60 (1H, d), 7.46 (1H, d), 7.36 (1H, s), 7.33 (1H, s), 7.32 (1H, s), 7.27 (1H, s), 7.15 (1H, d), 2.50 (3H, s), 2.42 (s, 6H), 2.41 (s, 6H), 2.07 (s, 6H), 2.06 ppm (s, 6H).

The carboxylate form of the complex was obtained by dissolving the chloride salt of [(tmbpy)<sub>2</sub>Ru<sup>II</sup>(Meby-COOH)]<sup>2+</sup> in a minimal amount of water. The pH was adjusted to ~10 with sodium hydroxide,

(25) Peek, B. M.; Ross, G. T.; Edwards, S. W.; Meyer, G. J.; Meyer, T. J.; Erickson, B. W. *Int. J. Pept. Protein Res.* **1991**, *38*, 114.

(26) Opperman, K. A.; Mecklenburg, S. L.; Meyer, T. J. *Inorg. Chem.* **1994**, *33*, 5295.

**Table 1.** Rates for Unimolecular and Bimolecular Electron Transfer for Donor–Acceptor Complexes with Amidinium–Carboxylate and Dicarboxylic Acid Dimer Bridges in Dichloromethane at 22 °C

salt bridge complex	$\Delta G^\circ/\text{eV}^a$	$k_{\text{ET}}/10^9 \text{ M}^{-1} \text{ s}^{-1}$	$k_{\text{PCET}}/10^6 \text{ s}^{-1}$
	−0.14	1.2	8.4
	−0.34	3.3	310
	−0.23	3.2	43

<sup>a</sup> Excited state redox potentials of the  $[(\text{tmbpy})_2\text{Ru}^{\text{II}}(\text{Mebypy-amidinium})]^{3+}$ ,  $[(\text{tmbpy})_2\text{Ru}^{\text{II}}(\text{Mebypy-COO}^-)]^+$ , and  $[(\text{tmbpy})_2\text{Ru}^{\text{II}}(\text{Mebypy-COOH})]^{2+}$  donors were determined from the simple thermodynamic relation:  $E_{1/2}(*\text{Ru}^{\text{III/II}}) = \Delta G_{\text{es}}^\circ - E_{1/2}(\text{Ru}^{\text{III/II}})$ , where  $E_{1/2}(\text{Ru}^{\text{III/II}})$  and  $E_{1/2}(*\text{Ru}^{\text{III/II}})$  are the ground state and excited state  $\text{Ru}^{\text{III/II}}$  reduction potentials, respectively. The excited state free energies ( $\Delta G_{\text{es}}^\circ$ ) of 2.23, 2.11, and 2.22 eV were determined from eqs 3 and 4, and the  $\text{Ru}^{\text{III/II}}$  reduction potentials of 1.05, 1.02, and 1.05 eV were measured by cyclic voltammetry ( $\text{CH}_2\text{Cl}_2$  containing 0.1 M tetrabutylammonium hexafluorophosphate as supporting electrolyte), respectively. Reduction potentials of 3,5-dinitrobenzoate and 3,5-dinitrobenzamidinium were measured to be  $-1.04$  and  $-0.85$  V vs SCE, respectively. Protonation of the acceptors was estimated to facilitate reduction by 0.1 V.

and dropwise addition of a saturated solution of sodium hexafluorophosphate yielded an orange precipitate. The precipitate was filtered onto a fine frit and washed with water. Because the complex is slightly soluble in aqueous solution, a minimal amount of water should be used for washing ( $3 \times 5$  mL). The gummy, air-dried solid was washed with copious amounts of anhydrous ethyl ether to remove any vestiges of water, thereby yielding a microcrystalline solid:  $^1\text{H}$  NMR ( $\text{DMSO-}d_6$ ) 8.85 (1H, s), 8.73 (1H, s), 8.57 (2H, s), 8.55 (2H, s), 7.66 (1H, d), 7.60 (1H, d), 7.45 (1H, d), 7.29 (5H, m), 2.50 (3H, s), 2.41 (9H, s), 2.39 (3H, s), 2.07 (6H, s), 2.06 ppm (12H, s).

**Synthesis of Tetrabutylammonium 3,5-Dinitrobenzoate.** Twenty-three milliliters of a 1.0 M tetrabutylammonium hydroxide–methanol solution was added via buret to a flask containing 3,5-dinitrobenzoic acid (5.0 g, 23 mmol). The mixture was stirred until the acid was completely dissolved. A viscous oil remained upon removal of the methanol under reduced pressure. The oil was dissolved in freshly distilled benzene, and 10 g of basic alumina was added to the solution, which was stirred for 10 min and filtered. The filtrate was freeze-dried to yield the product as a fluffy white solid: yield 8.5 g, 81%; MS 212.1  $m/z$ ;  $^1\text{H}$  NMR ( $\text{DMSO-}d_6$ ) 8.90 (s, 2H), 8.75 (1H, s), 3.20, (8H, s), 1.57 (8H, p) 1.28, (8H, s), 0.89 ppm (12H, t);  $^{13}\text{C}$  NMR ( $\text{DMSO-}d_6$ ) 162.97, 147.46, 146.00, 128.25, 117.91, 57.551, 23.11, 19.22, 13.42 ppm.

**Synthesis of 3,5-Dinitrobenzamidinium Tetraphenylborate.** The chloride salt of 3,5-dinitrobenzamidinium (0.5 g, 2.03 mmol), which has previously been prepared by Creary,<sup>27</sup> was dissolved in a minimal amount water, and residual solid was removed by filtering through a fine frit. An aqueous solution of sodium tetraphenylborate (1.0 g, 2.92 mmol) was added to the filtrate to afford a lemon yellow precipitate. This solid was filtered, washed with water ( $5 \times 15$  mL), dried in air, and washed with anhydrous ethyl ether ( $5 \times 15$  mL). The metathesis reaction proceeded with nearly quantitative conversion: MS 210.0  $m/z$ ;  $^1\text{H}$  NMR ( $\text{DMSO-}d_6$ ) 9.59 (s, 4H), 9.15, (s, 1H), 9.10, (s, 2H), 7.24 (s, 8H), 6.97 (t, 8H), 6.83 ppm (t, 4H);  $^{13}\text{C}$  NMR 164.44, 163.79, 163.13, 162.48, 162.21, 147.87, 135.64, 131.07, 129.31, 125.37, 123.03, 121.60 ppm.

(27) Creary, X. *J. Org. Chem.* **1993**, *58*, 7700.

**Physical Methods.** Electronic absorption spectra were recorded on a Cary 17 absorption spectrometer, retrofitted with the hardware and software design modifications of On-Line Systems Inc. Electrospray mass spectrometric (ES/MS) analyses were obtained with a Finnegan MAT (San Jose, CA) quadrupole mass spectrometer using a  $\text{CH}_3\text{CN}$  mobile phase. A  $\text{CH}_3\text{CN}$  solution of the sample was infused directly into the vaporization nozzle of the electrospray ion source at a flow rate of  $3 \text{ mL min}^{-1}$ . Nitrogen was used as the nebulizing gas at a pressure of 35 psi. NMR spectra were recorded on a Varian VXR 300, and samples were thermostated at 298(0.2) K.

Association constants for **1** and **2** were determined by measuring the  $^1\text{H}$  NMR chemical shift of amidinium protons by titrating  $\text{DMSO-}d_6$  solutions of the appropriate amidinium compound with varying amounts of the complementary carboxylate compound. Thus, for **1**, the hexafluorophosphate salt of  $[(\text{tmbpy})_2\text{Ru}^{\text{II}}(\text{Mebypy-amH}^+)]^{3+}$  (6.3 mM) was titrated with tetrabutylammonium 3,5-dinitrobenzoate, whereas 3,5-dinitrobenzamidinium tetraphenylborate (2.9 mM) was titrated with  $[(\text{tmbpy})_2\text{Ru}^{\text{II}}(\text{Mebypy-COO}^-)]^+$  ( $\text{PF}_6^-$  salt).

Emission spectra were obtained by exciting freeze/pump/thaw degassed solutions of the Ru(II) polypyridyl complexes at 435.8 nm with the 200 W Hg/Xe lamp of a spectrometer designed and constructed at Michigan State University.<sup>28</sup> The instrument was recently modified to include photon-counting detection, supported by associated hardware and software.<sup>29</sup> The modifications did not alter the optical path, which comprised a 338 Hz chopper and a 0.22 m double monochromator (3 mm/3 mm) for excitation wavelength selection; an Oriel interference filter was used for additional wavelength discrimination prior to the monochromator. Emitted light from samples was detected by a dry-ice-cooled Hamamatsu R3104 gated photon-counting photomultiplier tube mounted to a 0.5 m single monochromator (2.5 mm/2.5 mm). Emission quantum yields were determined by referencing the emission intensity from  $\text{CH}_2\text{Cl}_2$  solutions (22 °C) of the Ru(II) polypyridyl complex to  $[\text{Ru}(\text{bpy})_3][(\text{PF}_6)_2]$  in  $\text{CH}_2\text{Cl}_2$  ( $\phi_e = 0.029$ );<sup>30</sup> appropriate

(28) Shin, Y.-g. K.; Miskowski, V. M.; Nocera D. G. *Inorg. Chem.* **1990**, *29*, 2308.

(29) Saari, E. A., to be published.

(30) Kalyanasundaram, K. *Photochemistry of Polypyridine and Porphyrin Complexes*; Academic Press: London, 1992; Chapter 6.

corrections for differences in sample and quantum yield standard absorbances were applied.<sup>31</sup>

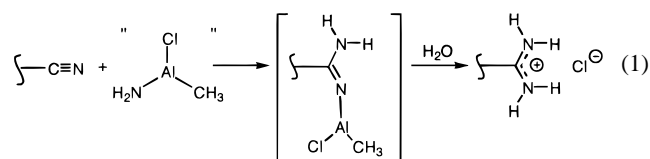
Bimolecular and unimolecular electron transfer rate constants for **1** and **3** were determined from emission lifetime decay curves. Isotropic emission was collected on a previously described lifetime instrument.<sup>32</sup> An excitation wavelength of 504 nm was achieved by pumping a H<sub>2</sub> Raman shift cell with the 355 nm third harmonic of a Quanta-Ray DCR-2 Nd:YAG laser. Decay traces were captured by a TEK DSA 602A digitizing signal analyzer oscilloscope, which averaged 512 data sets for each lifetime measurement. The shorter lifetimes of **2** were not amenable to nanosecond time-resolved laser measurements. In this case, lifetime decays were measured by time-correlated single-photon counting on an instrument that has previously been described.<sup>33</sup>

Lifetime measurements were made on freeze/pump/thaw degassed solutions of the Ru(II) polypyridyl complex contained in a sample chamber consisting of a Suprasil spectroscopic 1 cm high vacuum cell connected to a 10 mL round-bottom flask. The two chambers of the cell were isolated by a high-vacuum Teflon stopcock; a second stopcock isolated the entire cell from the environment. For quencher additions, the sample solution was isolated in the 1 cm cell by the Teflon stopcock. A stock solution of quencher ( $2 \times 10^{-3}$  M) was micropipetted into the round bottom flask, the cell was sealed, and the solvent was removed under high vacuum. The solid quencher was mixed with the Ru(II) solution by simply opening the intervening stopcock that separated the two chambers. Supramolecules **1** and **2** were formed by mixing the respective salts of the acceptor and donor.

Electrochemical measurements were performed on a workstation comprising an EG&G PAR 173 potentiostat/galvanostat, a PAR 175 universal programmer, and a PAR 179 digital coulometer. The output of the digital coulometer was fed directly into a Houston Instrument Model 2000 X-Y recorder. Cyclic voltammograms were measured at room temperature by using a Pt disk working electrode ( $A = 0.08$  cm<sup>2</sup>) for the Ru(II) complexes and a glassy carbon electrode for the acceptors, Pt wire auxiliary, and a Ag wire pseudoreference potential in a standard H-cell configuration. Redox couples for the Ru(II) polypyridyl complexes (2–5 mM), 3,5-dinitrobenzamidine (PF<sub>6</sub><sup>-</sup> salt), and 3,5-dinitrobenzoic acid were determined on CH<sub>2</sub>Cl<sub>2</sub> solutions containing 0.1 M tetrabutylammonium (TBA<sup>+</sup>) hexafluorophosphate as supporting electrolyte. Redox couples were referenced to SCE by using a ferrocenium–ferrocene internal standard of 0.307 V vs SCE.<sup>34</sup>

## Results and Discussion

Table 1 displays the donor–acceptor salt bridge complexes that we have designed for comparative PCET kinetics. The 4'-methyl-2,2'-bipyridine (Me bpy) ligand with amidine and carboxylate functionalities is derived from the aldehyde, which may be converted to the nitrile following Olah's procedure<sup>35</sup> in good yields. Conversion of the aldehyde to the carboxylic acid is accomplished under standard oxidation conditions.<sup>25</sup> The amidine group is afforded by adapting Garigipati's method<sup>36</sup> of reacting nitrile with Weinreb's amide transfer reagent, methylaluminum(III) chloramide:



In our hands, the amidinium chloride is directly obtained from

(31) Lakowicz, J. R. *Principles of Fluorescence Spectroscopy*; Plenum Press: New York, 1983; Chapters 2.7, 2.8.

(32) Zaleski, J. M.; Chang, C. K.; Nocera, D. G. *J. Phys. Chem.* **1993**, *97*, 13206.

(33) Bowman, L. E.; Berglund, K. A.; Nocera, D. G. *Rev. Sci. Instrum.* **1993**, *64*, 338.

(34) Bard, A. J.; Faulkner, L. R. *Electrochemical Methods. Fundamentals and Applications*; John Wiley: New York, 1980.

(35) Olah, G. A.; Keumi, T. *Synthesis* **1979**, 112.

(36) Garigipati, R. A. *Tetrahedron Lett.* **1990**, 31, 1969.

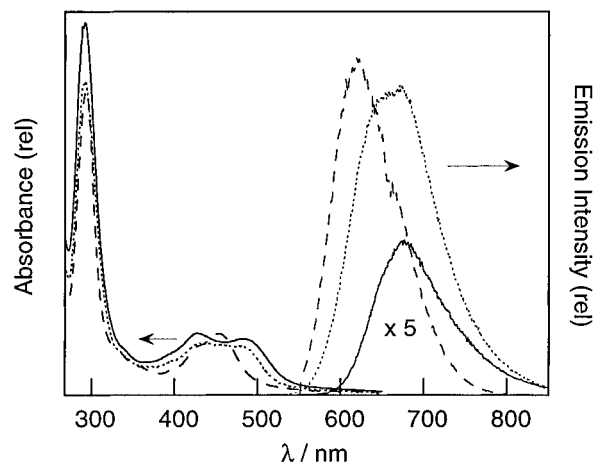
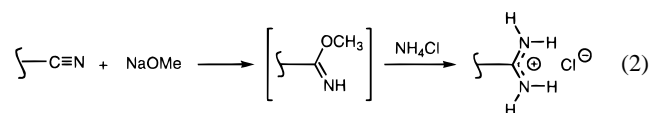


**Figure 1.** Electronic absorption and emission spectra of (a) [(tmbpy)<sub>2</sub>Ru<sup>II</sup>(Me bpy-amH<sup>+</sup>)]<sup>3+</sup> (—), [(tmbpy)<sub>2</sub>Ru<sup>II</sup>(Me bpy-COO<sup>-</sup>)]<sup>+</sup> (---), and [(tmbpy)<sub>2</sub>Ru<sup>II</sup>(Me bpy-COOH)]<sup>2+</sup> (···) in CH<sub>2</sub>Cl<sub>2</sub> at 22 °C.

this conversion. Alternatively, for the polypyridine modification, we have obtained 4-methyl-2,2'-bipyridine-4'-amidinium (Me bpy-amH<sup>+</sup>) chloride in higher yields by the base-catalyzed reaction of the nitrile with methoxide to afford the imidate ester, which smoothly reacts with ammonium chloride<sup>37</sup> as follows:



The metal complexes are afforded by standard reactions of the modified Me bpy ligands with the *cis*-dichloride, [(tmbpy)<sub>2</sub>RuCl<sub>2</sub>].<sup>38</sup> The electronic spectra of [(tmbpy)<sub>2</sub>Ru<sup>II</sup>(Me bpy-amH<sup>+</sup>)]<sup>3+</sup>, [(tmbpy)<sub>2</sub>Ru<sup>II</sup>(Me bpy-COO<sup>-</sup>)]<sup>+</sup>, and [(tmbpy)<sub>2</sub>Ru<sup>II</sup>(Me bpy-COOH)]<sup>2+</sup>, shown in Figure 1, are typical of Ru(II) polypyridyl complexes.<sup>30</sup> Absorption profiles are dominated by a high-energy  $\pi-\pi^*$  intraligand absorption band and a split, lower energy  $d\pi-\pi^*$  MLCT absorption band. Nonaqueous solutions of the complexes exhibit a strong red luminescence, as indicated by the normalized emission profiles of Figure 1. Luminescence decay curves exhibit monoexponential behavior, and a fit of the data yields lifetimes of 860, 1030, and 770 ns for [(tmbpy)<sub>2</sub>Ru<sup>II</sup>(Me bpy-amH<sup>+</sup>)]<sup>3+</sup>, [(tmbpy)<sub>2</sub>Ru<sup>II</sup>(Me bpy-COO<sup>-</sup>)]<sup>+</sup>, and [(tmbpy)<sub>2</sub>Ru<sup>II</sup>(Me bpy-COOH)]<sup>2+</sup>, respectively.

The Ru(II) carboxylate and amidinium complexes readily form the salt bridge with the corresponding acceptor. Complexes **1** and **2** have been thoroughly characterized by NMR. Figure 2 shows the <sup>1</sup>H NMR spectral changes resulting for the association of [(tmbpy)<sub>2</sub>Ru<sup>II</sup>(Me bpy-amH<sup>+</sup>)]<sup>3+</sup> to 3,5-dinitrobenzoate (3,5-DNBCOO<sup>-</sup>) in DMSO-*d*<sub>6</sub>. As observed previously for guanidinium–carboxylate salt bridges,<sup>39</sup> signatures of the salt bridge are the concentration-dependent downfield shift of amidinium protons involved in hydrogen bonding (NH<sub>ax</sub>) and an insensitivity of the chemical shift for the amidinium protons external to the salt bridge (NH<sub>eq</sub>). The chemical shift of the NH<sub>ax</sub> protons varies by 2.4 ppm upon their hydrogen-bonding association to the carboxylate, whereas the chemical shift of the NH<sub>eq</sub> protons varies by <0.3 ppm over the same concentration range. A nonlinear least-squares fit of chemical shift of the hydrogen-bonded amidinium protons vs the carboxylate

(37) Schaefer, F. C.; Peters, G. A. *J. Org. Chem.* **1961**, *26*, 412.

(38) Sullivan, B. P.; Salmon, D. J.; Meyer, T. J. *Inorg. Chem.* **1978**, *12*, 3334.

(39) Müller, G.; Riede, J.; Schmidtchen, P. *Angew. Chem., Int. Ed. Engl.* **1988**, *27*, 1516.

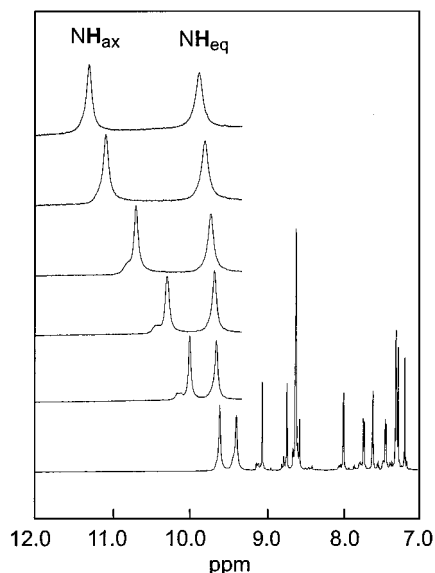


**Figure 2.** Spectral changes of  $^1\text{H}$  NMR spectrum of  $[(\text{tmbpy})_2\text{Ru}^{\text{II}}(\text{bpy}-\text{amH}^+)]^{3+}$  with added tetrabutylammonium 3,5-dinitrobenzoate. Selected spectra are shown upon addition of 3,5-dinitrobenzoate at concentrations 0.0, 2.3, 3.7, 6.6, 10.3, and 13.9, mM in  $\text{DMSO}-d_6$  (bottom to top). The  $^1\text{H}$  resonances of the bipyridines appear between 7.0 and 9.2 ppm; two broad singlets flanking 9.5 ppm signify the  $^1\text{H}$  resonances of the axial (internal) and equatorial (external) amidinium protons.

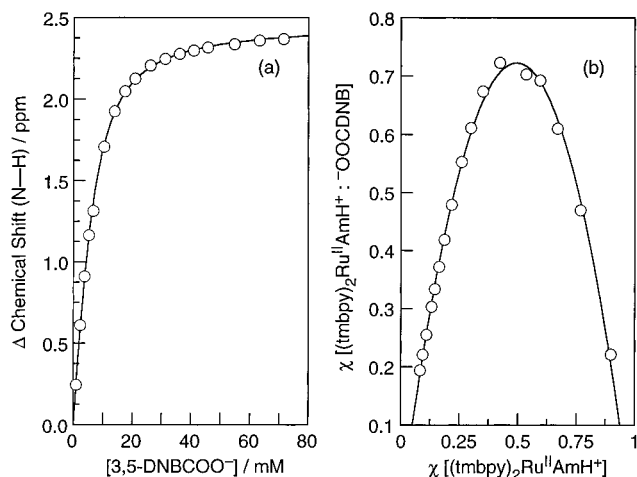


**Figure 3.** (a) Plot of the chemical shift of the resonances shown in Figure 2 for  $[(\text{tmbpy})_2\text{Ru}^{\text{II}}(\text{bpy}-\text{amH}^+)]^{3+}$  and additional resonances of the amidinium protons hydrogen-bonded to carboxylate versus concentration of carboxylate from 0.0 to 80 mM. (b) Job's plot of the relative salt bridge complex concentration vs the mole fraction of  $[(\text{tmbpy})_2\text{Ru}^{\text{II}}(\text{bpy}-\text{amH}^+)]^{3+}$  (6.3 mM) as the concentration of 3,5-DNBCOO $^-$  is varied from 0.0 to 80 mM.

concentration (Figure 3a), as described by Wilcox,<sup>40</sup> yields an association constant ( $K_{\text{assoc}}$ ) of  $386 \text{ M}^{-1}$ . A 1:1 stoichiometry of the supramolecule complexes is established by the Job's plot<sup>41</sup> of the  $^1\text{H}$  NMR titration data reproduced in Figure 3b, which shows that the optimal formation of **1** occurs at equimolar concentrations of the amidinium and carboxylate (i.e., a 0.5 mole fraction). This is definitive evidence for the 1:1 stoichiometry of the amidinium–carboxylate salt bridge. Similar behavior is observed for **2** (see Supporting Information). The

(40) Wilcox, C. S. In *Frontiers in Supramolecular Organic Chemistry and Photochemistry*; Schneider, H.-J., Durr, H., Eds.; VCH: Weinheim, 1991; p 123.

(41) Albert, J. S.; Goodman, M. S.; Hamilton, A. D. *J. Am. Chem. Soc.* **1995**, *117*, 1143.

$\text{NH}_{\text{eq}}$  resonance (9.53 ppm) of 3,5-dinitrobenzamidinium (3,5-DNBamH $^+$ ) exhibits an insignificant shift upon the addition of  $[(\text{tmbpy})_2\text{Ru}^{\text{II}}(\text{Mebpy}-\text{COO}^-)]^+$  ( $\Delta\text{ppm} < 0.2$  over 10 mM), while  $\text{NH}_{\text{ax}}$  varies by 2.5 ppm over the 10 ppm concentration range. The larger shift of  $\text{NH}_{\text{eq}}$  resonances over the smaller concentration range as compared to that for **1** is indicative of the higher association constant of  $2297 \text{ M}^{-1}$  for **2** in DMSO. This greater association constant of **2** is consistent with the electron-withdrawing nitro groups conferring a decreased basicity of the carboxylate group on 3,5-DNB, resulting in a weaker hydrogen-bonding interaction for **1**. In less polar solvents, the association constant greatly increases. The low solubility of **1** and **2** in  $\text{CH}_2\text{Cl}_2$  (the solvent in which electron transfer kinetics were determined, *vide infra*) precludes reliable determination of  $K_{\text{assoc}}$  by NMR titration experiments. However, the binding can conveniently be monitored by infrared or electronic absorption spectroscopy. For **1**, the split MLCT transition coalesces upon salt bridge formation, with an isosbestic point maintained at 487 nm. A Benesi–Hildebrand fit of the absorption maxima with added carboxylate yields  $K_{\text{assoc}} = 5.6 \times 10^5 \text{ M}^{-1}$ . Shifts in the electronic absorption spectra for **2** are not as pronounced. In this case, an association constant of  $> 10^7 \text{ M}^{-1}$  was measured by infrared spectroscopy.

The design of the excited state structure of the Ru(II) polypyridyl complex is crucial to a proper kinetics study of the electron transfer reactions of **1–3**. The electron transfer reaction to the 3,5-dinitrobenzene acceptor of **1–3** is initiated by laser excitation of the metal-to-ligand charge transfer (MLCT) transition of the Ru(II) polypyridyl complex. Two potential reaction pathways arise for the oxidative quenching reaction, depending on the energetics of the MLCT excited state. For the case where the lowest energy MLCT excited state is localized on the salt-bridge-modified Mebpy ligand, photoexcitation will place the transferring electron directly into the PCET pathway. Alternatively, a lowest energy MLCT excited state involving the ancillary polypyridine ligand will remove the excited electron from the PCET reaction pathway. Indeed, we have confronted this issue in our earlier studies of the oxidative quenching of  $[(\text{bpy})_2\text{Ru}^{\text{II}}(\text{Mebpy}-\text{X})]^{n+}$  ( $\text{X} = \text{COO}^-$ ,  $n = 1$ ;  $\text{X} = \text{amH}^+$ ,  $n = 3$ ).<sup>24a</sup> In the absence of tetramethyl substitution of the bipyridine rings, the MLCT excited states involving the ancillary bpy and the Mebpy-amH $^+$  and Mebpy-COO $^-$  ligands are close in energy, thereby obscuring a comparative PCET study owing to the presence of the two competing reaction pathways.

The relative energies of the relevant MLCT excited states for systems **1–3** may be evaluated by analyzing the emission profiles of the various homoleptic complexes as follows:<sup>26</sup>

$$\Delta G_{\text{es}}^{\circ} = E_0 + \chi \quad (3)$$

$$\chi = (\Delta\bar{\nu}_{0,1/2})^2 (16k_{\text{B}}T \ln 2)^{-1} \quad (4)$$

where the excited state energy ( $\Delta G_{\text{es}}^{\circ}$ ) is related to the energy of the luminescence maximum ( $E_0$ ) and the reorganization energy ( $\chi$ ) containing solvent and low-frequency modes, which are treated classically and related to the full width at half-maximum,  $\Delta\bar{\nu}_{0,1/2}$  for a single vibronic component. The relation of the spectroscopic energy to a free energy arises from negligible pressure–volume work (and, hence, the energy is primary enthalpic)<sup>42</sup> and small electronic entropic contributions accompanying excited state production.<sup>43</sup> Measured values of

(42) Hupp, J. T.; Neyhart, G. A.; Meyer, T. J.; Kober, E. M. *J. Phys. Chem.* **1992**, *96*, 10820.

(43) Balzani, V.; Scandola, F. *Supramolecular Photochemistry*; Ellis Horwood: New York, 1991; Chapter 2.7.2.

$E_o = 14,843 \text{ cm}^{-1}$  and  $\Delta\bar{\nu}_{1/2} = 2476 \text{ cm}^{-1}$  for Ru(II) tris-(Mebpy-amH<sup>+</sup>) and  $E_o = 15,359 \text{ cm}^{-1}$  and  $\Delta\bar{\nu}_{1/2} = 1826 \text{ cm}^{-1}$  for Ru(II) tris(Mebpy-COO<sup>-</sup>) complex yield excited state energies ( $E_{o,o}$ ) of 2.17 and 2.08 eV, respectively, as compared to  $E_{o,o} = 2.56 \text{ eV}$  of Ru(tmbpy)<sub>3</sub><sup>2+</sup>.<sup>26</sup> The destabilization of the  $d\pi \rightarrow \pi^*$ (tmbpy) MLCT by nearly 0.4 eV with regard to the MLCT excited states of Mebpy-amH<sup>+</sup> and Mebpy-COO<sup>-</sup> ensures that photoexcitation of 1–3 cleanly promotes the transferring electron onto the Mebpy ligand, from where it can smoothly advance to the dinitrobenzoic acceptor.

Consistent with these excited state energetics, the Ru(II) excited state undergoes electron transfer reactions with unbound and bound acceptor. The luminescence from the [(tmbpy)<sub>2</sub>Ru<sup>II</sup>(Mebpy-COO<sup>-</sup>)]<sup>+</sup> bound to benzamidinium and [(tmbpy)<sub>2</sub>Ru<sup>II</sup>(Mebpy-amidinium)]<sup>3+</sup> bound to benzoate is long-lived, with observed excited state lifetimes of 1200 and 470 ns, respectively. Owing to the large association constants of 1 and 2 in CH<sub>2</sub>Cl<sub>2</sub>, these lifetimes are independent of benzamidinium and benzoate at concentrations greater than that of the metal complex. Conversely, the presence of the 3,5-DNB electron-accepting group leads to efficient quenching of the Ru(II) excited state luminescence for 1–3. For each system, biphasic decay kinetics are observed for the quencher concentration range investigated. One component of the emission decay is clearly dependent on the concentration of quencher, whereas the other component remains concentration-independent; these data are presented in Figure 4. The concentration-dependent lifetimes obey typical linear Stern–Volmer quenching kinetics, and the rate constants for the bimolecular reactions of the respective constituents of supramolecule assemblies are listed in Table 1. The bimolecular reaction at low concentrations likely involves complexed quencher and free Ru(II) complex as a result of the high association constants of the supramolecule assemblies 1 and 2. The bimolecular rate constants for 1–3 accord well with the kinetics of equiexergonic bimolecular reactions between Ru<sup>II</sup> tris(polypyridyl) and nitroaromatic quenchers.<sup>44</sup> Of greater relevance to PCET are the attendant concentration-independent rate constants, which we attribute to the unimolecular electron transfer of the associated complexes.<sup>45</sup> The striking result of these data listed in Table 1 is that the electron transfer rate constant through 1 is considerably slower than that for its switched interface congener, 2. The differences in the unimolecular rate constants for 1 and 2 reveal that the rate of electron transfer depends significantly on the salt bridge and its orientation with respect to the electron transfer pathway.

The slower rate of 1 may have several origins. In 1, the permanent dipole ( $\delta^+\delta^-$ ) of the salt bridge is in the direction of electron transfer, whereas in 2, electron transfer opposes the dipole. Internal electrostatic fields affect the rates of electron transfer by altering the driving force of reaction relative to the isolated constituents.<sup>46–48</sup> By using typical bond distances of Ru(bpy)<sub>3</sub><sup>2+</sup>, DNB, and the amidinium–carboxylate salt bridge,

(44) Bock, C. R.; Connor, J. A.; Gutierrez, A. R.; Meyer, T. J.; Whitten, D. G.; Sullivan, B. P.; Nagle, J. K. *J. Am. Chem. Soc.* **1979**, *101*, 4815.

(45) Assuming a diffusion-controlled on rate of  $10^9 \text{ M}^{-1} \text{ s}^{-1}$  for these systems, from the measured equilibrium constants for 1 and 2, off rates of  $2 \times 10^3$  and  $10^2 \text{ s}^{-1}$ , respectively, are expected for these systems. Of course, the pertinent equilibrium is with electronically excited Ru(II) complex and not the ground state complex, as measured by absorption spectroscopy. Notwithstanding, the largest  $\Delta pK_a$  changes for Ru(II) polypyridyl complexes between ground and excited states are 3; for instance, blys directly appended with carboxylic acids exhibit  $\Delta pK_a$ s of 2.5 (see ref 30). Hence, the observed intramolecular electron transfer decay rates well exceed equilibration rates, and intramolecular electron transfer occurs for a static complex. This is not the case for 3, however, where the off rates are expected to be commensurate with the electron transfer kinetics. For this system, the interpretation of the observed PCET rate constant reported in Table 1 is complicated by a dynamic equilibrium between acceptor and donor.

(46) Galoppini, E.; Fox, M. A. *J. Am. Chem. Soc.* **1996**, *118*, 2299.

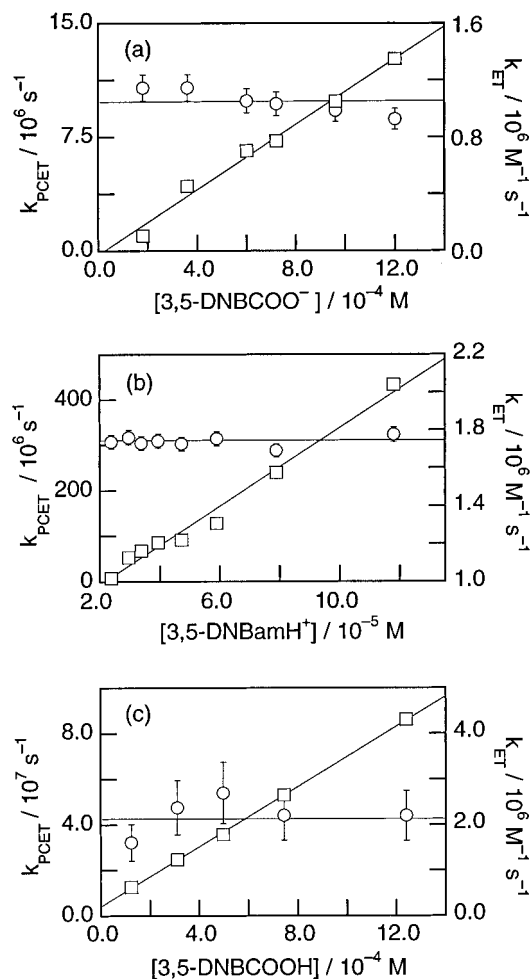


**Figure 4.** Plot of the concentration-independent (○) and concentration-dependent (□) observed rate constants for the quenching of (a) [(tmbpy)<sub>2</sub>Ru<sup>II</sup>(bpy-amH<sup>+</sup>)]<sup>3+</sup> (0.064 mM) by 3,5-DNB COO<sup>-</sup>, (b) [(tmbpy)<sub>2</sub>Ru<sup>II</sup>(Mebpy-COO<sup>-</sup>)]<sup>+</sup> (0.10 mM) by 3,5-DNB amH<sup>+</sup>, and (c) [(tmbpy)<sub>2</sub>Ru<sup>II</sup>(Mebpy-COOH)]<sup>2+</sup> (0.060 mM) by 3,5-DNB COOH in CH<sub>2</sub>Cl<sub>2</sub> at 22 °C.

we calculate a 0.37 V (less favorable for 1) field-induced difference between the driving force for intramolecular electron transfer ( $\Delta E_C = e^2/\epsilon r^{49}$ ). This thermodynamic attenuation of the electron transfer rate constant for 1 may be further augmented by a greater reorganization energy associated with the salt bridge. In 1, accompanying proton transfer (from the Ru<sup>II</sup> amidinium donor to the carboxylate acceptor) can stabilize the charge of the electron as it develops on the acceptor. In this case, since the proton charge is strongly coupled to the solvent dipoles, as with the electron, charge shift within the salt bridge may be accompanied by significant solvent polarization, thereby giving rise to additional Franck–Condon factors. This is not the case for 2. Here, the proton is already residing on the acceptor, and hence it is likely to remain upon the arrival of the electron. Finally, differences in H-bonding strengths of the asymmetric interfaces may be manifested in differences in electronic coupling efficiencies.<sup>50</sup> The electron-withdrawing nitro groups will stabilize the negative charge on the carboxylate, resulting in a weaker hydrogen bond in 1 and, hence, a correspondingly weaker electronic coupling pathway.

(47) Stanley, R. J.; King, B.; Boxer, S. G. *J. Phys. Chem.* **1996**, *100*, 12052.

(48) Heller, B. A.; Holten, D.; Kirmaier, C. *Science* **1995**, *269*, 940.

(49) Scherer, T.; van Stokkum, I. M. H.; Brouwer, A. M.; Verhoeven, J. *W. J. Phys. Chem.* **1994**, *98*, 10539.

(50) Gray, H. B.; Winkler, J. R. *Annu. Rev. Biochem.* **1996**, *65*, 537.

Our results show that intervening salt bridges can profoundly mediate the rates of intramolecular electron transfer. Unlike a symmetric interface, the salt bridge can significantly affect the rate of electron transfer from contributions of the electrostatic potential, Franck–Condon factors, and electronic coupling arising from the asymmetric charge distribution. Such effects will be present in any biological system where the developing charge resulting from proton motion coupled to the electron transfer pathway is not compensated (e.g., proton pumps, oxygen activation). Current studies are underway to begin disentangling the contributions of the different PCET mechanisms for electron transfer through asymmetric interfaces.

**Acknowledgment.** The financial support of the National Institutes of Health (GM 47274) is gratefully acknowledged. J.A.R. acknowledges support from the Carl H. Brubaker, Jr., Fellowship in Chemical Sciences.

**Supporting Information Available:**  $^1\text{H}$  NMR spectra of  $[(\text{tmbpy})_2\text{Ru}^{\text{II}}(\text{Mebpy-COO}^-)]^+$  with varying concentrations of acceptor 3,5-DNBamH $^+$ , Job's plot, and fit of the chemical shift data to obtain  $K_{\text{assoc}}$  (4 pages). See any current masthead page for ordering and Internet access instructions.

JA970176+